Evaluation of multisource precipitation input for hydrological modeling in an alpine basin: a case study from the Yellow River Source Region (China)

Pengfei Gu[1], Gaoxu WANG[2], Guodong Liu[1], Yongxiang Wu[2], Hongwei Liu[2], Xi Jiang[2], and Tao Liu[2]

[1]Sichuan University
[2]Nanjing Hydraulic Research Institute

September 24, 2021

Abstract

Alpine basins are essential to the conservation of water resources. However, they are typically poorly gauged and inaccessible, owing to the harsh prevailing environment and complex terrain. To investigate the influences of different precipitation inputs on hydrological modeling in alpine basins, two representative satellite precipitation products [Tropical Rainfall Measuring Mission (TRMM) and Integrated Multi-Satellite Retrievals for GPM (IMERG)] and two reanalysis precipitation products [China Meteorological Assimilation Driving Datasets for the SWAT model (CMADS) and Climate Forecast System Reanalysis (CFSR)] in the Yellow River Source Region (YRSR) were selected for evaluation and hydrological verification against gauge-observed data (GO). Results indicates that the accuracy of these precipitation products in the warm season is higher than that in the cold season, and IMERG has the best performance, followed by CMADS, CFSR, and TRMM. TRMM seriously overestimates high rainfall of greater than 10 mm/day. CFSR overestimates moderate precipitation events of 1–10 mm/d, while CMADS underestimates the effects of precipitation events of 1–20 mm/d. Models using the GO as input yielded satisfactory performance during 2008–2013, and precipitation products have poor simulation results. Although the model using IMERG as input yielded unsatisfactory performance during 2014–2016, this did not affect the use of IMERG as a potential data source for YRSR. After bias correction, the quality of CFSR improves significantly with R2 and NSE increasing by 0.25 and 0.31 at Tangnaihai station, respectively. Model driven by the combination of GO and CMADS precipitation performed the best in all scenarios (R2 = 0.77, NSE = 0.72 at Tangnaihai station; R2 = 0.53, NSE = 0.48 at Jimai station). These results can provide reference data, and research ideas, for improved hydrological modeling of alpine basins.

Introduction

Accurate precipitation data are key for the hydrological modeling (Duan*et al* ., 2019a; Monteiro *et al* ., 2016; Strauch *et al* ., 2012; Villarán, 2014). However, due to the sparsity of many gauge networks and the large spatio-temporal variabilities of precipitation events (Lu *et al* ., 2018; Zhu *et al* ., 2016), obtaining accurate precipitation data has always been challenging for scientists especially in alpine basins (Bhatta *et al* ., 2019; Hao *et al* ., 2016; Yuan *et al* ., 2018), which greatly hindered the research into hydrological simulation thereof (Tuo *et al* ., 2016). Satellite and reanalysis precipitation products provide an unprecedented opportunity to obtain precipitation data with high spatio-temporal resolution.

To date, many satellite and reanalysis precipitation products have been developed and released to the public, such as Global Precipitation Measurement (GPM) (Hou *et al* ., 2013), Tropical Rainfall Measuring

Mission (TRMM) (Huffman *et al* ., 2010a), Climate Hazards Group Infrared Precipitation with Station data (CHIRPS) (Funk *et al* ., 2015), China Meteorological Assimilation Driving Datasets for SWAT model (CMADS) (Meng *et al* ., 2019), Climate Forecast System Reanalysis (CFSR) (Saha *et al* ., 2010), *etc* . These products have the advantages of extensive coverage, high spatio-temporal resolution, and continuity of measurement (Bajracharya *et al* ., 2015; Prakash*et al* ., 2016): these have been widely applied in hydrological studies across many regions (Auerbach *et al* ., 2016; Awange*et al* ., 2019; Cao *et al* ., 2018; De Almeida Bressiani*et al* ., 2015; Duan *et al* ., 2019a; Fuka *et al* ., 2014; Roth and Lemann, 2016). The research on satellite and reanalysis precipitation products in hydrological model can be divided into two categories: one such that these products directly drive hydrological models to study and discuss the influence of precipitation data quality on the accuracy of hydrological simulations (Duan *et al* ., 2019b; Nhi *et al* ., 2018; Strauch *et al* ., 2012; Tuo *et al* ., 2016; Zhu *et al* ., 2016); the other aims at satellite and reanalysis precipitation data which are not performing well in hydrological modeling terms. The improvement of satellite and reanalysis precipitation data by different correction methods was studied and discussed (Deng *et al* ., 2019; Sheng *et al* ., 2017; Wang*et al* ., 2020). However, most of these literatures focus on low-altitude basins with dense in-situ gauge observation, because the satellite and reanalysis precipitation products in such areas are less affected by topography, making it is easier to evaluate and correct satellite and reanalysis precipitation data based on a large number of gauge-observed data (GO). Alpine basin areas are important in the conservation of water resources (Immerzeel *et al* ., 2009; Viviroli and Weingartner, 2004) and are sentinel outpost responding to climate change (Immerzeel *et al* ., 2010; Shakil *et al* ., 2015), such as on the Tibetan Plateau, known as "Asian Water Tower" (Immerzeel*et al* ., 2010). It is more meaningful to evaluate the quality of satellite and reanalysis precipitation products in an alpine basin and to mine precipitation products suitable for hydrological-runoff simulations thereof.

In recent years, many scholars (Deng *et al* ., 2019; Duan *et al* ., 2019a; Yuan *et al* ., 2018; Yw *et al* ., 2019) have discussed the hydrological application of satellite and reanalysis precipitation products in alpine basin. However, most of studies focus on the influence of precipitation product quality on hydrological simulation accuracy. Unfortunately, these research results show that the performance of precipitation data from sparse in-situ gauge observation stations in hydrological models is better than that of satellite and reanalysis precipitation products with high spatio-temporal resolution. Yuan *et al* . (2018) evaluated the quality of the TRMM Multi-satellite Precipitation Analysis 3B42V7 and the Integrated Multi-satellite Retrievals for GPM (IMERG) Final Run Version 05 precipitation products and their hydrological utilities in the Yellow River source region (YRSR), and found that the performance of GO is better than that of IMERG and TRMM precipitation data. In the Upper Gilge Abay basin, Duan *et al* . (2019a) evaluated the applicability of CHIRPS, TRMM, and CFSR in hydrological models by using the Soil and Water Assessment Tool (SWAT), still finding that the GO performed best. Use of ground-based rain gauge data is generally considered to be a more accurate method as this entails direct measurement of precipitation (Qin*et al* ., 2014). However, ground-based rain gauges are considered as point measurements within the common problem of the uneven distribution thereof (Chappell *et al* ., 2013), which may not effectively reflect the spatio-temporal variability of precipitation systems (Anagnostou *et al* ., 2009). Satellite and reanalysis precipitation products have the advantage of large coverage (Bajracharya*et al* ., 2015; Prakash *et al* ., 2016), which can supplement that precipitation information in areas without stations. How to coordinate the advantages of GO, satellite and reanalysis of precipitation data is the key to hydrological-runoff simulation in alpine basins.

The YRSR, with high solar radiation and a low temperature, is selected as a case study in the present research. Combined with the distributed hydrological model SWAT, two types of satellite precipitation products (TRMM and IMERG) and two types of reanalysis precipitation products (CMADS and CFSR) were statistically and hydrologically verified. This entailed: (1) Using GO to evaluate the quality of TRMM, IMERG, CMADS, and CFSR at grid and basin-scales; (2) The hydrological model is driven by precipitation data pre- and post-correction; (3) The hydrological model is driven by the combination of GO and satellite or reanalysis precipitation products, namely, for that area with GO we adopted GO, and in areas without GO we adopted satellite or reanalysis precipitation products. To the best of our knowledge, the hydrological evaluation of the combination of GO and satellite or reanalysis precipitation products in the YRSR has not

yet been reported. The results of this study have implications for improving water supply, flood forecasting, and ecosystem protection for alpine basins and their downstream regions.

Study area and data

2.1 Study area

The YRSR, with a drainage area of ˜122,000 km^2 accounting for ˜15% of the area of the Yellow River basin, is located in the north-east of the Qinghai-Tibetan Plateau (roughly ranging between 95°30'103deg30' E and 32deg30'36deg20 N). With elevations ranging from 2675 to 6253 m that decreases from the south-west to the north-east (**Fig. 1**). The YRSR belongs to a typical alpine climate (Xu and He, 2006), with intense sunshine and diurnal temperature changes. The rainfall predominately concentrates in the flood season (JuneOctober), accounting for ˜75% of the annual precipitation, and the snowfall is primarily concentrated from September to May (Hu *et al* ., 2011). Precipitation runoff is the predominate runoff pattern in the YRSR, accounting for ˜96% of the total runoff (Liu and Chang, 2005).

The YRSR has been selected as the study area duo to three reasons: (1) the YRSR provides fresh water to hundreds of millions of people downstream; (2) less impact of human activities with a total of approximately half a million inhabitants (Yuan *et al* ., 2015); (3) the YRSR is a sensitive zone in response to climate change (Junliang*et al* ., 2013).

2.2 Data

2.2.1 Precipitation dataset

Five types of precipitation datasets, namely, the GO, IMERG Final Run V6, TRMM 3B42RTV7, CMADS, and CFSR, were selected for this study (**Table 2**).

The GO was derived from the daily surface meteorological data of the China Meteorological Data Network. There are only 11 in-situ gauged observation stations in the YRSR, and most of them are distributed downstream, and there is only one Maduo station upstream [**Fig. 1(c)**].

The TRMM was launched in 1979 by the National Aeronautics and Space Administration (NASA) and the Japanese Aerospace Exploration Agency (JAXA) to provide satellite monitoring of global precipitation. In 2015, the TRMM mission ended, the instruments were shut down, and the spacecraft re-entered the Earth's atmosphere. In this study, the TRMM 3B42RTV7 daily precipitation product from 1 January 2008 to 31 December 2013 was used. The TRMM 3B42RTV7 precipitation products were generated by using the TRMM TMPA Version 7 algorithm (Huffman *et al* ., 2010b). To the best of our knowledge, the hydrological evaluation of TRMM 3B42RTV7 daily precipitation product in the YRSR has not yet been reported.

The Global Precipitation Measurement (GPM) was launched in February 2014 as the successor to TRMM providing the next generation of global precipitation products. The IMERG precipitation products were GPM's level-3 products produced by the IMERG algorithm. According to the timeliness of the various products, they can be divided into three levels: Early-Run, Late-Run, and Final-Run. The Final-Run product was generally considered to be more accurate in terms of its results than the quasi-real-time products (Early and Late Run) (Yang *et al* ., 2020). In this study, the IMERG Final-Run V6 daily precipitation product from 1 January 2008 to 31 December 2016 was selected, of which the precipitation data from January 2008 to February 2014 were calculated from the original remote sensing image of TMPA by IMERG algorithm. TRMM and IMERG precipitation products are currently two satellite precipitation products that were widely used in hydrological simulations (Duan *et al* ., 2019a; Nhi *et al* ., 2018; Yuan *et al* ., 2018).

The CMADS is a reanalysis dataset established using the China Meteorological Administration atmospheric assimilation system technology and multiple other scientific methods (Meng *et al* ., 2019). The CMADS was

completed over nine years (1 January 2008 to 31 December 2016). The application potential of CMADS in hydrological modeling has been verified in many watersheds in China (Li *et al* ., 2019; Meng*et al* ., 2019; Zhang *et al* ., 2020).

The CFSR is a reanalysis dataset developed by the National Centers for Environmental Prediction (NCEP) which was completed over 36 years (1 January 1974 to 31 December 2014) (Sorrel, 2010). CFSR in hydrological modeling is currently one of the most widely used reanalysis datasets with worldwide application (Ruan *et al* ., 2017; Yang *et al* ., 2020; Zhu *et al* ., 2015), owing to advantages such as its large time-scale, high-resolution spatial scale, and convenient data acquisition. CMADS and CFSR were both included on the ArcSWAT official website.

2.2.2 Other data

In addition to precipitation data, the following data are needed for model construction and verification:

(1) Digital Elevation Model (DEM): derived from SRTM_DEM data with a spatial resolution of 90 m provided by Geospatial Data Cloud (*http://www.gscloud.cn/*);

(2) Land use data: derived from the Chinese Academy of Sciences Resource and Environmental Science Data Center (*http://www.resdc.cn/*), Land-use data for China in 2015 (1980-2015), with a resolution of 1 km;

(3) Soil data: derived from the Harmonized World Soil Database (HWSD) constructed by Food and Agriculture Organization of the United Nations (FAO) and International Institute for Applied Systems Analysis (IIASA), with a resolution of 1 km (*http://westdc.westgis.ac.cn/*);

(4) Meteorological data: derived from the daily surface meteorological data of the China Meteorological Data Network (Version 3.0) (*http://data.cma.cn/*), including precipitation, maximum/minimum temperature, relative humidity, wind speed, and hours of sunshine. The solar radiation was calculated by use of the Angtrom-Prescott equation as detailed in Wu *et al* . (2012);

(5) Streamflow data: observed daily streamflow data at the Tangnaihai station (TNH) and Jimai station (JM) from 1 January 2008 to 31 December 2015 were collected from the Nanjing Hydraulic Research Institute, China.

Fig. 1(c) displays the spatial distribution of meteorological and hydrological stations. We set the projection coordinate system of the DEM, land use, and soil map to that of WGS_1984_Albers, with a central longitude of 100deg E and standard latitude (north latitude) of$\varnothing_1$=33.5deg, $\varnothing_2$=38deg.

Methodology

This study consists of two parts: in the first (precipitation product evaluation) we aimed to evaluate the quality of TRMM, IMERG, CMADS, and CFSR precipitation products at grid and watershed-scales based on GO; in the second (streamflow simulation evaluation), 12 precipitation scenarios were created to drive the hydrological model (**Table 2**). Scenarios S1 to S7 were used to study the runoff simulation effect of each precipitation dataset; Scenarios S8 and S9 were SWAT models driven by corrected precipitation data to study the influence of precipitation data correction on runoff simulation (**Section 4.2.2** describes the reasons for correcting only CMADS and CFSR precipitation data). Scenarios S10, S11, and S12 cover CMADS precipitation data combined with GO1, corrected CFSR precipitation data combined with GO1, and IMERG precipitation data combined with GO2, respectively: these were designed to study the effects of precipitation data combination on runoff simulation (**Section 4.2.3** describes the reasons for choosing these three combinations). The analysis process used herein is shown in **Fig. 2** .

3.1 Precipitation data evaluation

To quantitatively evaluate the accuracy of the TRMM, IMERG, CFSR, and CMADS precipitation products in the YRHR, the precipitation derived from the four precipitation products is directly compared with GO. Six statistical metrics, including the root mean square error (RMSE), percent bias (PBIAS), correlation coefficient (CC), probability of detection (POD), false alarm ratio (FAR), and critical success index (CSI), were utilized to evaluate the agreement between the GO and the four precipitation products. The calculation equations, units, ranges, and optimal values of the evaluation indicators are listed in **Table 3** .

3.2 SWAT model and model setting

The SWAT is a semi-distributed, physics-based eco-hydrological model, which runs in daily, monthly, or annual time steps (Arnold *et al* ., 1998), and has been widely used in hydrological processes (Grusson*et al* ., 2015), soil erosion (Song *et al* ., 2011), and nutrient transportation (Wang *et al* ., 2018). Previous studies have proven that dividing the YRSR into 25 (Liu *et al* ., 2018), 29 (Hao *et al* ., 2013), and 97 (Mengyaun *et al* ., 2019) sub-basins would yield reliable simulation results. Therefore, the YRSR was divided into 26 sub-basins to reduce unnecessary calculation. SWAT was originally developed to evaluate water resources in large agricultural basins, and was not designed to model heterogeneous mountain basins typical of the western United States (Fontaine *et al* ., 2002). Ten elevation zones (each covering an change in elevation of 500 m) were established in the present work, to divide each sub-basin to reduce the influence of topography on precipitation. According to previous research (Fontaine *et al* ., 2002; Zhenchun *et al* ., 2013), the snowfall temperature (SFTMP), snow melt base temperature (SMTMP), maximum melt rate for snow during year (SMFMX), minimum melt rate for snow during the year (SMFMN), snow pack temperature lag factor (TIMP), and minimum snow water content that corresponds to 100% snow cover (SNOCOVMX) in the snowmelt module have been adjusted to reduce the influence of snowmelt on the model (**Table 4**).

3.3 Parameter calibration and model evaluation

Calibration and uncertainty analyses of the simulation results from the model were performed using Sequential Uncertainty Fitting Version 2 (SUFI2) in the SWAT calibration and uncertainty program (SWAT-CUP) (Abbaspour *et al* ., 2015). According to previous studies on hydrological modeling in alpine basins (Bhatta *et al* ., 2019; Mengyaun *et al* , 2019; Shuai *et al* ., 2019; Zhenchun*et al* ., 2013), 30 sensitive parameters were initially selected. Sixteen parameters with the highest sensitivity were then selected using the Latin hypercube and one-factor-at-a-time sampling (LH-OAT) method for calibration (**Table 5**). Due to limitations of space, we do not present any analysis of the calibration parameters. According to Abbaspour (2015), the model was calibrated using three iterations with 400 simulations (necessitating a total of 1200 simulations during calibration) using the Nash-Sutcliffe Efficiency (NSE) (Nash and Sutcliffe, 1970) and coefficient of determination (R^2) as the objective function. The range of each parameter was modified after each iteration, according to both new parameters suggested by SWAT-CUP and their reasonable physical ranges. The criteria proposed by Moriasi *et al* (2015) was adopted to classify model performance into the respective categories, "very good" (NSE > 0.80; PBIAS < +-5%), "good" (0.70 < NSE [?] 0.80; +-5% [?] PBIAS < +-10%), "satisfactory" (0.50 < NSE [?] 0.70; +-10% [?] PBIAS < +-15%), and "unsatisfactory" (NSE [?] 0.50; PBIAS [?] +-15%).

3.4 Precipitation data pre-processing

Before modeling, we preprocessed the precipitation data:

(1) The numbers of grids or stations with precipitation products of TRMM, IMERG, CMADS, and CFSR located in the YRSR are 200, 1027, 198, and 122, respectively. Considering that SWAT only uses data from the one weather station closest to the centroid of the sub-basin (Masih *et al* ., 2011; Villaran, 2014). It is impractical to divide the watershed into 1027 sub-watersheds and correspond thereto on a one-by-one basis.

Therefore, virtual weather stations were constructed for each sub-basin (Ruan *et al* ., 2017; Tuo*et al* ., 2016). The specific methods are as follows:

- Based on the ArcGIS platform, satellite raster or reanalysis station precipitation data falling in each sub-basin were extracted;
- The arithmetic average method was used to calculate the areal rainfall of each sub-basin, giving precipitation data pertaining to each virtual precipitation station;
- The centroid of each sub-basin is the location of the virtual precipitation station [**Fig. 1 (c)**].

(2) Considering that the starting period of SWAT-CUP calibration must be a whole year, the periods of coincidence of CMADS (1 January 2008 to 31 December 2016) and CFSR (1 January 1974 to 31 December 2014) data are only six years (1 January 2008 to 31 December 2013), deducting the warm-up period of the SWAT model (12 years), the final simulation time will be shorter (45 years), which does not reflect the quality of the data. Therefore, we added meteorological data from 1 January 2008 to 31 December 2010 and 1 January 2006 to 31 December 2007 for the warm-up of the SWAT model, so that the data time-span used for the simulation becomes six years (1 January 2008 to 31 December 2013).

Results

4.1 Evaluation of multi-precipitation products

4.1.1 Evaluation at basin-scale

According to **Fig. 5** , except TRMM, the data from other precipitation products show a decreasing trend from south-east to north-west, which is consistent with the results of Hu *et al*(2011). Compared with GO, the precipitation data of IMERG and IMERG_T are the closest, while the precipitation data of TRMM and CFSR are significantly overestimated, and the precipitation data of CMADS are significantly underestimated. Several literatures (Ghodichore *et al* ., 2018; Graham *et al* ., 2019; Saha *et al* ., 2014) found that reanalysis precipitation products obviously overestimated or underestimated observed precipitation.

The further to reflect the difference between the precipitation products and the GO, the PBIAS, CC, and RMES of the precipitation products and the GO were counted on a monthly time-scale. Based on **Fig. 4** , the PBIAS values of TRMM, IMERG_T, IMERG, CMADS, and CFSR were characterized by low warm season precipitation and high cold season precipitation. TRMM precipitation data were underestimated in January and February, and overestimated at other times, especially from October to December. IMERG_T precipitation data were underestimated in the rainy season (MayNovember) and overestimated in the dry season (DecemberApril). IMERG precipitation data were underestimated in the dry season (DecemberApril), but IMERG performed best in observing precipitation in the rainy season (average PBIAS = -2.26%). CMADS precipitation data were underestimated in other months except December. The precipitation data of CFSR overestimated the precipitation in all months. Except IMERG, the CC values of other precipitation products also show characteristics of being lower in the warm season and higher in the cold season, among which CFSR has the best correlation with GO (average CC = 0.73), while CMADS, TRMM, IMERG_T, and IMERG perform poorly, with mean CC values of 0.23, 0.01, -0.01, and -0.28, respectively. However, the RMSE values of five types of precipitation products show seasonal characteristics related to the greater precipitation in the warm season and lower precipitation in the cold season in the YRSR (Hu *et al* ., 2011). IMERG precipitation products have the smallest deviation, with RMSE average of 13.71 mm, followed by CMADS (17.35 mm), CFSR (21.32 mm), IMERG_T (32.42 mm), and TRMM (47.89 mm).

To reveal whether different precipitation products can capture precipitation events within various precipitation intensity groups, we use the probability density function approach to evaluate the daily precipitation intensity (PI), divided PI into nine bins (0 [?] PI $<$ 0.1, 0.1 [?] PI $<$ 1, 1 [?] PI $<$ 5, 5 [?] PI $<$ 10, 10 [?] PI $<$ 15, 15 [?] PI $<$ 20, 20 [?] PI $<$ 30, 30 [?] PI $<$ 40, and PI [?] 40). Based on**Fig. 5** , IMERG, IMERG_T,

CMADS, and CFSR can correctly capture precipitation classifications, but TRMM overestimates high rainfall of > 10 mm/day. IMERG and CFSR overestimate the intensity of all precipitation events, especially CFSR, which significantly overestimates moderate precipitation events of 110 mm/d. The precipitation underestimation by CMADS is mainly concentrated within the range of 120 mm/d, while events within the range of 0.11 mm/d are overestimated.

4.1.2 Evaluation at grid-scale

According to **Fig. 6** , the qualities of the TRMM, IMERG_T, IMERG, CMADS, and CFSR were generally better in the south-east than in the north-west. The north-western areas are covered with snow all year round, owing to their high altitude and higher latitude. This leads to poor-quality precipitation observations in this area (Mark *et al* ., 2016; Noh *et al* ., 2009). The overestimation of TRMM is the largest with PBIAS of 33.11% to 59.74%, and this gradually increases from downstream to upstream. The precipitation data of CFSR were overestimated except for the station at Dari, while CMADS precipitation data were underestimated except for the station at Maqu. IMERG precipitation data were overestimated in the downstream area and underestimated upstream. Compared with satellite precipitation products (CC of 0.090.40), the reanalysis precipitation products (CC of 0.340.58) have a better correlation with GO. The RMSE values of five precipitation products were large in the south-east and small in the north-west. According to the statistical indicators pertaining to various precipitation products, the overall performance of CMADS precipitation products is the best, with PBIAS of 27.22%2.48%, CC of 0.430.58, and RMSE of 2.684.96 (mm/d), followed by IMERG, CFSR, IMERG_T, and TRMM.

IMERG_T and TRMM have the same detection index value [**Figs. 7(a) and (b)**], and the specific reason for this is given in**Section 2.2.1** , so here we only analyzed TRMM. According to**Fig. 7** , the four precipitation products have high detection rates (POD [?] 0.60), of which CFSR performs best (POD [?] 0.90), followed by IMERG (0.67 [?] POD [?] 0.82), CMADS (0.63 [?] POD) [?] 0.84), and TRMM (0.60 [?] POD [?] 0.70). FAR values of four precipitation products increase with latitude. Among the four precipitation products, TRMM shows the highest false alarm ratio (0.40 [?] FAR [?] 0.57), followed by IMERG (0.40 [?] FAR [?] 0.57), CFSR (0.29 [?] FAR [?] 0.57) and CMADS (0.30 [?] FAR [?] 0.48). CFSR has the highest comprehensive forecasting ability, with a CSI of 0.480.69, followed by CMADS and IMERG, and TRMM exhibits the worst comprehensive forecasting ability. According to the detection indicators of various precipitation products, the overall performance of CFSR precipitation products is the best, with a POD of 0.900.98, FAR of 0.290.51, and CSI of 0.48-0.69, followed by CMADS, IMERG, and TRMM.

4.2 Evaluation of hydrological simulations

4.2.1 Results of streamflow simulation using different precipitation datasets

According to **Fig. 8** , the runoff simulation results of Scenario S1 are the best overall, with R^2 and NSE values of 0.85/0.75, 0.84/0.51 in the calibration/validation periods at TNH and 0.81/0.57, 0.80/0.39 in the calibration/validation periods at JM. Scenario S6 performed second best, and in the validation periods (R^2 = 0.78, NSE = 0.53 at TNH;R^2 = 0.64, NSE = 0.53 at JM) yielded the satisfactory performance and outperformed Scenario S1, but it performed poorly in the calibration periods. Scenario S6 underestimates the runoff during the dry season, owing to the CMADS precipitation data being underestimated (**Fig. 4**). The runoff simulation results of Scenarios S3 and S7 were significantly overestimated, and neither TNH nor JM reached a satisfactory performance, especially with respect to Scenario S3 at JM. The reason for this is that the precipitation data of TRMM and CFSR were overestimated (**Fig. 4**), and the precipitation data of TRMM overestimate the upstream precipitation [**Figs 3(c) and 6(b)**].

Based on **Figs 8 and 9** , the runoff simulation results of Scenario S5 were significantly better than those of Scenario S3, but slightly worse than in Scenario S2. In calibration periods, scenario S2 (R^2 = 0.76, NSE = 0.75 at TNH;R^2 = 0.77, NSE = 0.70 at JM) and S5 (R^2 = 0.70, NSE = 0.65 at TNH;R^2 = 0.66, NSE = 0.66 at JM), the runoff simulation results yielded a satisfactory performance, but the performance of the

two in the validation periods was extremely poor (NSE [?] 0.26). This may be due to the short time-series of precipitation data in Scenarios S2 and S5, and the limited number of calibration times of parameters, which leads to significant differences in the performance of simulation results in the calibration and validation periods. In summary, the runoff simulation results based on GO performed best overall, followed by IMERG, CMADS, CFSR, IMERG_T, and TRMM. IMERG and CMADS precipitation products can be used in this data-scarce alpine region.

4.2.2 Results of streamflow simulation using corrected precipitation datasets

As mentioned in **Section 4.1** , the GO and the reanalyzed precipitation products have a high correlation at basin and grid-scales, but the correlation with the satellite precipitation products is poor (**Figs 4 and 6**). Therefore, we only corrected the precipitation data of CMADS and CFSR. We used GO to perform daily-scale regression analysis on CMADS and CFSR precipitation data at basin-scale, owing to scarcity of data in the YRSR. Comparing the fitting effects of different functions, it is found that R^2 of the resulting cubic polynomial is the highest. According to cubic polynomial fitting,R^2 of CMADS is 0.827, andR^2 of CFSR is 0.934 (**Fig. 10**).

Fig. 11 shows that the corrected CFSR precipitation data has improved the simulation results at TNH. The simulation results have changed from unsatisfactory to satisfactory, and theR^2 (NSE) value during the calibration and validation periods increased (increased) by 0.28 (0.34) and 0.22 (0.27), respectively. However, the overall performance of CMADS after correction remains unsatisfactory because the correlation between GO and CFSR precipitation data is better than that of CMADS (**Fig. 4**). Compared with TNH, the corrected CMADS and CFSR precipitation data generate no improvements in runoff model results of JM, and the simulated results remain unsatisfactory.

4.2.3 Results of streamflow simulation using combined precipitation datasets

By using R^2 and NSE indicators, it is found that the simulated results of IMERG and CMADS precipitation data are close to, or even better than, the GO in calibration or validation periods (**Figs 8 and 9**). The performance of CFSR precipitation data after correction is better (**Fig. 11**). Therefore, we choose the combination of CMADS, CFSR_C, and IMERG precipitation data and GO, corresponding to Scenarios S10, S11, and S12. The spatial distribution of precipitation stations is shown in **Fig. 1(b)** .

According to **Table 2** , the overall performance of Scenario S10 combining GO and CMADS is the best, and the simulation results at TNH resulted in good performance ($R^2 = 0.77$, NSE = 0.72), which is superior to Scenario S1 ($R^2 = 0.80$, NSE = 0.68) and Scenario S8 ($R^2 = 0.59$, NSE = 0.50). Although the simulation results at JM yielded unsatisfactory performance, they were close to being deemed satisfactory (calibration periods: $R^2 = 0.50$, NSE = 0.48; validation periods: $R^2 = 0.55$, NSE = 0.47). The runoff simulation results of Scenarios S11 and S12 are not as good as those of Scenarios S1 and S2, but slightly better than those of Scenarios S5 and S9.

5. Discussion

Precipitation is the key variable input for hydrological modeling and the main source of error in simulation results (Duan *et al* ., 2019a; Ruan *et al* ., 2017). Currently, many satellite and reanalysis precipitation products have been widely used in hydrological simulation in areas lacking observation (Bhatta *et al* ., 2019; Bitew and Gebremichael, 2010; Tang *et al* ., 2019). However, the quality of precipitation products is obviously different in different zones, owing to different climatic regions, seasonal cycles, and land types (Wang *et al* ., 2020). Before further use of satellite and reanalysis of precipitation products, it is necessary to evaluate the quality of these precipitation products. The error in satellite precipitation products usually stems from the weak relationship between precipitation rate and remote sensing signals (Bitew and Gebremichael, 2010), satellite revisit time (B *et al* ., 2013), and retrieval algorithm (Yan *et al* ., 2020). For reanalysis of

precipitation products, the uncertainties and errors mainly come from data sources, interpolation algorithms, and data assimilation systems (Zhu *et al* ., 2015).

According to the results, the accuracy of TRMM, IMERG, CMADS, and CFSR in the warm season is higher than that in the cold season, and IMERG has the best performance, followed by CMADS, CFSR, and TRMM. This is mainly because snowfall is the main precipitation in winter in the YRSR (Hu*et al* ., 2011). Although most satellite retrieval algorithms perform quite well in rainfall estimation, the accuracy of snowfall estimation is still not high, especially on snow-covered or frozen land surfaces (Cai *et al* ., 2015; Noh *et al* ., 2009; Villarini*et al* ., 2009). Alijanian *et al* . (2017) and Condom *et al* . (2011) reported that TRMM precipitation products cannot express the spatio-temporal variability of precipitation over high-altitude, complex terrain. IMERG, as a newer generation of TRMM precipitation products, are more sensitive to the capture of solid precipitation events (Yang*et al* ., 2020), due to the more advanced GPM microwave Imager sensor and the Dual-frequency Precipitation Radar onboard the GPM satellites. Most scientific literatures reported that IMERG has a better performance in alpine basin (Mou and Santo, 2018; Yuan *et al* ., 2015). In addition, high-latitude regions respond strongly to climate change, which poses a huge challenge to satellite precipitation observations (Mark *et al* ., 2016). Tian and Peters-Lidard (2010) reported that the satellite precipitation products have large uncertainty in high latitudes (beyond +- 40deg). By contrast, the reanalysis precipitation products is less affected by high-latitude and high-altitude (Beck *et al* ., 2017; Serreze *et al* ., 2005; Yong *et al* ., 2014). At the grid scale, among the four precipitation products, CMADS has the best performance for precipitation observation (**Fig. 6**), and CFSR has the best performance for precipitation events (**Fig. 7**).

Due to the scarcity of in-situ gauged observation stations in the alpine basin, it is not comprehensive to evaluate the performance of precipitation products based on statistical methods. Hydrological simulation verification is a supplementary method for the evaluation of precipitation products (Deng *et al* ., 2019; Guoqiang *et al* ., 2015). Using GO from even sparse in-situ gauged observation stations resulted in better performance in runoff simulation than using all four precipitation products, which is consistent with the previous research results (Yuan *et al* ., 2015). Among the four precipitation products, IMERG has the best performance in runoff simulation, followed by CMADS, CFSR, and TRMM. TRMM seriously overestimated runoff simulation with NSE values of -1.86 and -11.93 at TNH and JM, respectively. This is mainly due to the poor quality of precipitation products in near real time (Tekeli and Fouli, 2016). In general, the simulation results of runoff at TNH are better than those at JM. There are two main reasons: one is the high altitude in the basin above JM and the large snow-covered, which will increase the microwave reflectivity on the land surface, thereby mask the drop in microwave signal due to scattering (Harpold *et al* ., 2017; Yong *et al* ., 2014); Second, in-situ gauged observation stations in the YRSR are mostly distributed downstream, and there are only two precipitation stations in the basin above JM (**Fig. 1**). Compared with the model driven by a single precipitation dataset, the model driven by the combination of GO and satellite or reanalysis precipitation products has better performance, especially Scenario S10 performed the best in all scenarios (R^2 = 0.77, NSE = 0.72 at TNH;R^2 = 0.53, NSE = 0.48 at JM). This is probably because CMADS precipitation products consider more gauge-based precipitation than CFSR and IMERG (Meng *et al* ., 2016). These results can provide reference data, and research ideas, for improved hydrological modeling of alpine basins.

6. Conclusions

The overall objective of this study was to evaluate the hydrological application potential of TRMM, IMERG, CMADS, and CFSR in the YRSR. The major findings of this study are summarized as follows.

(1) At the basin-scale, the TRMM, IMERG, CMADS, and CFSR have higher detection accuracy in the warm season, and the PBIAS and CC values of each precipitation product are characterized by small warm season and large cold season values. Among the four precipitation products, IMERG had the smallest deviation (average RMSE = 13.71 mm), while CFSR had the best correlation (average CC = 0.73)

(2) At the grid scale, among the four precipitation products, CMADS has the best performance for precipitation observation, with PBIAS of -27.22%2.48 %, CC of 0.430.58, and RMSE of 2.684.96 (mm/d), followed by IMERG, CFSR, and TRMM. CFSR has the best performance for precipitation events, with POD of 0.900.98, FAR of 0.290.51, and CSI of 0.480.69, followed by CMADS, IMERG and TRMM.

(3) Taken together, IMERG has the best performance, followed by CMADS, CFSR, and TRMM. TRMM severely overestimated high rainfall of $>$ 10 mm/day. CFSR obviously overestimated moderate precipitation events of 110 mm/d, while CMADS underestimated the precipitation events of 120 mm/d.

(4) Models using the GO as input resulted in satisfactory performance during 20082013, and precipitation products have poor simulation results. The results of simulation using CMADS significantly underestimated the runoff during the dry season, but the performance in the validation periods ($R^2 = 0.78$, NSE = 0.53 at TNH; $R^2 = 0.64$, NSE = 0.53 at JM) was best among those scenarios analyzed. The runoff simulated using TRMM and CFSR is significantly overestimated, especially when using TRMM. Although the model using IMERG as input yielded unsatisfactory performance during 20142016, it did not affect the use of IMERG as a potential data source for YRSR.

(5) After bias correction, the quality of CFSR improves significantly with increases to R^2 and NSE of 0.25 and 0.31 at TNH, respectively. SWAT model driven by the combination of GO and CMADS precipitation was the best across all scenarios. The simulation results at TNH yielded satisfactory performance ($R^2 = 0.77$, NSE = 0.72). Although the simulation results at JM yielded an unsatisfactory performance, they were close to being deemed satisfactory ($R^2 = 0.53$, NSE = 0.48).

In summary, although the satellite and reanalysis precipitation products represented by TRMM and CFSR have been widely used in hydrological modeling, the quality of these products could be significantly improved when applied to alpine basins. In contrast, IMERG has a better performance in observing solid precipitation due to the more advanced GPM microwave imager sensor and the dual-frequency precipitation radar mounted on the GPM satellites (Yang *et al* ., 2020). The findings of this assessment provide valuable reference and feedback for satellite and reanalysis precipitation product development for use in alpine basins. In addition, snowfall is the main form of precipitation in the YRSR from September to May, however, such an assessment was not fulfilled due to the lack of snowfall observation site, a task that warrants investigation and inclusion in future research.

Acknowledgement

This study was supported by National Key Research and Development Program of China (Grant No. 2016YFC0401005, 2016YFA0601703) and Nation Nature Science Foundation of China (Grant No. 91847301, 92047203, 42075191, 52009080). Acknowledgement for the data support form “National Earth System Science Data Center, National Science & Technology Infrastructure of Chia. (http://www.geodata.cn)”

Declaration of Competing Interest

All authors declare that there is no financial or personal interest or belief that could affect our objectivity. We declare that we have no conflict of interest.

References

Abbaspour, K., 2015. SWAT-Calibration and uncertainty programs (CUP). Neprashtechnology.Ca. https://doi.org/10.1007/s00402-009-1032-4

Alijanian, M., Rakhshandehroo, G.R., Mishra, A.K., Dehghani, M., 2017. Evaluation of satellite rainfall climatology using CMORPH, PERSIANN-CDR, PERSIANN, TRMM, MSWEP over Iran. Int. J. Climatol. 37.

Anagnostou, E.N., Maggioni, V., Nikolopoulos, E.I., Meskele, T., Hossain, F., Papadopoulos, A., 2009. Benchmarking High-Resolution Global Satellite Rainfall Products to Radar and Rain-Gauge Rainfall Estimates. IEEE Trans. Geosci. Remote Sens.

Arnold, J.G., Srinivasan, R., Muttiah, R.S., Williams, J.R., 1998. Large area hydrologic modeling and assessment part I: Model development. J. Am. Water Resour. Assoc. https://doi.org/10.1111/j.1752-1688.1998.tb05961.x

Auerbach, D.A., Easton, Z.M., Walter, M.T., Flecker, A.S., Fuka, D.R., 2016. Evaluating weather observations and the Climate Forecast System Reanalysis as inputs for hydrologic modelling in the tropics. Hydrol. Process. https://doi.org/10.1002/hyp.10860

Awange, J.L., Hu, K.X., Khaki, M., 2019. The newly merged satellite remotely sensed, gauge and reanalysis-based Multi-Source Weighted-Ensemble Precipitation: Evaluation over Australia and Africa (1981–2016). Sci. Total Environ. https://doi.org/10.1016/j.scitotenv.2019.03.148

B, V.T.A., C, R.R., A, Z.B., B, A.D.R.A., 2013. Hydrological evaluation of satellite-based rainfall estimates over the Volta and Baro-Akobo Basin. J. Hydrol. 499, 324–338.

Bajracharya, S.R., Palash, W., Shrestha, M.S., Khadgi, V.R., Duo, C., Das, P.J., Dorji, C., 2015. Systematic evaluation of satellite-based rainfall products over the brahmaputra basin for hydrological applications. Adv. Meteorol. https://doi.org/10.1155/2015/398687

Beck, H.E., Vergopolan, N., Ming, P., Levizzani, V., Wood, E., 2017. Global-scale evaluation of 22 precipitation datasets using gauge observations and hydrological modeling. Hydrol. Earth Syst. Sci. 21, 6201–6217.

Bhatta, B., Shrestha, S., Shrestha, P.K., Talchabhadel, R., 2019. Evaluation and application of a SWAT model to assess the climate change impact on the hydrology of the Himalayan River Basin. Catena. https://doi.org/10.1016/j.catena.2019.104082

Bitew, M.M., Gebremichael, M., 2011. Assessment of satellite rainfall products for streamflow simulation in medium watersheds of the Ethiopian highlands. Hydrol. Earth Syst. Sci. 15, 1147–1155. https://doi.org/10.5194/hess-15-1147-2011

Bitew, M.M., Gebremichael, M., 2010. Assessment of high-resolution satellite rainfall for streamflow simulation in medium watersheds of the East African highlands. Hydrol. Earth Syst. Sci. Discuss. 7.

Cai, Y., Jin, C., Wang, A., Guan, D., Wu, J., Yuan, F., Xu, L., 2015. Spatio-Temporal Analysis of the Accuracy of Tropical Multisatellite Precipitation Analysis 3B42 Precipitation Data in Mid-High Latitudes of China. PLoS One 10.

Cao, Y., Zhang, J., Yang, M., Lei, X., Guo, B., Yang, L., Zeng, Z., Qu, J., 2018. Application of SWAT model with CMADS data to estimate hydrological elements and parameter uncertainty based on SUFI-2 algorithm in the Lijiang River basin, China. Water (Switzerland). https://doi.org/10.3390/w10060742

Chappell, A., Renzullo, L.H., Raupach, T.J., Haylock, M., 2013. Evaluating geostatistical methods of blending satellite and gauge data to estimate near real-time daily rainfall for Australia. J. Hydrol. https://doi.org/10.1016/j.jhydrol.2013.04.024

Condom, T., Rau, P., Espinoza, J.C., 2011. Correction of TRMM 3B43 monthly precipitation data over the mountainous areas of Peru during the period 1998–2007. Hydrol. Process. 25, 1924–1933.

De Almeida Bressiani, D., Srinivasan, R., Jones, C.A., Mendiondo, E.M., 2015. Effects of different spatial and temporal weather data resolutions on the stream flow modeling of a semi-arid basin, Northeast Brazil.

Int. J. Agric. Biol. Eng. https://doi.org/10.3965/j.ijabe.20150803.970

Deng, P., Zhang, M., Bing, J., Jia, J., Zhang, D., 2019. Evaluation of the GSMaP_Gauge products using rain gauge observations and SWAT model in the Upper Hanjiang River Basin. Atmos. Res. 219, 153–165. https://doi.org/10.1016/j.atmosres.2018.12.032

Duan, Z., Tuo, Y., Liu, J., Gao, H., Song, X., Zhang, Z., Yang, L., Mekonnen, D.F., 2019a. Hydrological evaluation of open-access precipitation and air temperature datasets using SWAT in a poorly gauged basin in Ethiopia. J. Hydrol. 569, 612–626. https://doi.org/10.1016/j.jhydrol.2018.12.026

Duan, Z., Tuo, Y., Liu, J., Gao, H., Song, X., Zhang, Z., Yang, L., Mekonnen, D.F., 2019b. Hydrological evaluation of open-access precipitation and air temperature datasets using SWAT in a poorly gauged basin in Ethiopia. J. Hydrol. https://doi.org/10.1016/j.jhydrol.2018.12.026

Fontaine, T.A., Cruickshank, T.S., Arnold, J.G., Hotchkiss, R.H., 2002. Development of a snowfall-snowmelt routine for mountainous terrain for the soil water assessment tool (SWAT). J. Hydrol. 262, 209–223. https://doi.org/10.1016/S0022-1694(02)00029-X

Fuka, D.R., Walter, M.T., Macalister, C., Degaetano, A.T., Steenhuis, T.S., Easton, Z.M., 2014. Using the Climate Forecast System Reanalysis as weather input data for watershed models. Hydrol. Process. https://doi.org/10.1002/hyp.10073

Funk, C., Peterson, P., Landsfeld, M., Pedreros, D., Verdin, J., Shukla, S., Husak, G., Rowland, J., Harrison, L., Hoell, A., 2015. The climate hazards infrared precipitation with stations—a new environmental record for monitoring extremes. Sci. Data 2, 150066.

Ghodichore, N., Vinnarasi, R., Dhanya, C.T., Roy, S.B., 2018. Reliability of reanalyses products in simulating precipitation and temperature characteristics over India. J. Earth Syst. Sci. 127.

Graham, R.M., Cohen, L., Ritzhaupt, N., Segger, B., Hudson, S.R., 2019. Evaluation of Six Atmospheric Reanalyses over Arctic Sea Ice from Winter to Early Summer. J. Clim. 32, 4121–4143.

Grusson, Y., Sun, X., Gascoin, S., Sauvage, S., Raghavan, S., Anctil, F., Sachez-Perez, J.M., 2015. Assessing the capability of the SWAT model to simulate snow, snow melt and streamflow dynamics over an alpine watershed. J. Hydrol. 531, 574–588. https://doi.org/10.1016/j.jhydrol.2015.10.070

Guoqiang, T., Zhe, L., Xianwu, X., Qingfang, H., Bin, Y., 2015. A study of substitutability of TRMM remote sensing precipitation for gauge-based observation in Ganjiang River basin. Adv. Water Sci. https://doi.org/10.14042/j.cnki.32.1309.2015.03.005

Hao, Guo, Sheng, Chen, Anming, Bao, Ali, Behrangi, Yang, Hong, 2016. Early assessment of Integrated Multi-satellite Retrievals for Global Precipitation Measurement over China. Atmos. Res.

Hao, Z., Zhang, Y., Yang, C., Li, J., Thondup, D., 2013. Effects of topography and snowmelt on hydrologic simulation in the Yellow River's source region. Shuikexue Jinzhan/Advances Water Sci.

Harpold, A.A., Kaplan, M.L., Zion, K.P., Timothy, L., Mcnamara, J.P., Seshadri, R., Rina, S., Steele, C.M., 2017. Rain or snow: hydrologic processes, observations, prediction, and research needs. Hydrol. Earth Syst. Sci. 21, 1–48.

Hou, A.Y., Kakar, R.K., Neeck, S., Azarbarzin, A., Kummerow, C.D., Kojima, M., Oki, R., Nakamura, K., Iguchi, T., 2013. The Global Precipitation Measurement Mission. Bull. Am. Meteorol. Soc. 95, 701–722.

Hu, Y., Maskey, S., Uhlenbrook, S., Zhao, H., 2011. Streamflow trends and climate linkages in the source region of the Yellow River, China. Hydrol. Process. 25, 3399–3411. https://doi.org/10.1002/hyp.8069

Huffman, G.J., Adler, R.F., Bolvin, D.T., Nelkin, E.J., 2010a. The TRMM Multi-Satellite Precipitation Analysis (TMPA). j hydrometeor.

Huffman, G.J., Bolvin, D.T., Nelkin, E.J., Wolff, D.B., Adler, R.F., Gu, G., Yang, H., Bowman, K.P., Stocker, E.F., 2010b. The TRMM Multisatellite Precipitation Analysis (TMPA): Quasi-Global, Multiyear, Combined-Sensor Precipitation Estimates at Fine Scales. Satellite Rainfall Applications for Surface Hydrology.

Immerzeel, W.W., Beek Van, L.P.H., Bierkens, M.F.P., 2010. Climate change will affect the Asian water towers. Science 328, 1382–5.

Immerzeel, W.W., Droogers, P., Jong, S.M.D., Bierkens, M., 2009. Large-scale monitoring of snow cover and runoff simulation in Himalayan river basins using remote sensing. Remote Sens. Environ. 113, 40–49.

Junliang, J., Guoqing, W., Guishan, L., Ruimin, H., Qingye, H., 2013. Responses of hydrology and water resources to the climate change in the Yellow River source region. J. Arid L. Resour. Environ. 27, 137–143. https://doi.org/10.13448/j.cnki.jalre.2013.05.029

Li, Y., Wang, Y., Zheng, J., Yang, M., 2019. Investigating spatial and temporal variation of hydrological processes in western China driven by CMADS. Water (Switzerland) 11. https://doi.org/10.3390/w11030435

Liu, J., Shanguan, D., Liu, S., Ding, Y., 2018. Evaluation and hydrological simulation of CMADS and CFSR reanalysis datasets in the Qinghai-Tibet Plateau. Water (Switzerland). https://doi.org/10.3390/w10040513

Liu, X., Chang, X., 2005. A Summary of Study on RunoffVar iations in Source Reg ion of the Yellow R iver. YELLOW RIVER 27, 6–12. https://doi.org/1000 - 1379(2005)02 - 0006 -03

Lu, X., Wei, M., Tang, G., Zhang, Y., 2018. Evaluation and correction of the TRMM 3B43V7 and GPM 3IMERGM satellite precipitation products by use of ground-based data over Xinjiang, China. Environ. Earth Sci. 77, 209.

Mark, Richardson, Matthew, Lebsock, Matthew, Christensen, Graeme, Stephens, David, Bolvin, 2016. Status of high-latitude precipitation estimates from observations and reanalyses. J. Geophys. Res. D. Atmos. JGR 121, 4468–4486.

Masih, I., Maskey, S., Uhlenbrook, S., Smakhtin, V., 2011. Assessing the Impact of Areal Precipitation Input on Streamflow Simulations Using the SWAT Model1. Jawra J. Am. Water Resour. Assoc. 47, 179–195.

Meng, X., Shi, C., Liu, S., Wang, H., Lei, X., Liu, Z., Ji, X., Cai, S., Zhao, Q., 2016. CMADS Datasets and Its Application in Watershed Hydrological Simulation: A Case Study of the Heihe River Basin. Pearl River 37, 1–19. https://doi.org/10.3969/j.issn.1001-9235.2016.07.001

Meng, X., Zhang, X., Yang, M., Wang, H., Chen, J., Pan, Z., Wu, Y., 2019. Application and evaluation of the China Meteorological Assimilation Driving Datasets For The Swat Model (CMADS) in poorly gauged regions in Western China. Water (Switzerland) 11, 1–28. https://doi.org/10.3390/w11102171

Mengyaun, W., Hongwei, X., Jie, Z., Yiping, W., 2019. Runoff simulation of the Yellow River source region based on SWAT model. J. Qinghai Univ. 37, 39–46. https://doi.org/10.13901/j.cnki.qhwxxbzk.2019.01.007

Monteiro, J., Strauch, M., Srinivasan, R., Abbaspour, K., Gucker, B., 2016. Accuracy of grid precipitation data for Brazil: application in river discharge modelling of the Tocantins catchment. Hydrol. Process. 30.

Moriasi, D.N., Gitau, M.W., Pai, N., Daggupati, P., 2015. Hydrologic and water quality models: Performance measures and evaluation criteria. Trans. ASABE 58, 1763–1785. https://doi.org/10.13031/trans.58.10715

Mou, L.T., Santo, H., 2018. Comparison of GPM IMERG, TMPA 3B42 and PERSIANN-CDR satellite precipitation products over Malaysia. Atmos. Res. 202, 63–76.

Nash, J.E., Sutcliffe, J. V, 1970. River flow forecasting through conceptual models part I — A discussion of principles - ScienceDirect. J. Hydrol. 10, 282–290.

Nhi, P., Khoi, D.N., Hoan, N.X., 2018. Evaluation of five gridded rainfall datasets in simulating streamflow in the upper Dong Nai river basin, Vietnam. Int. J. Digit. Earth 1–17.

Noh, Y., Liu, G., Jones, A.S., H Aa R, T., 2009. Toward snowfall retrieval over land by combining satellite and in situ measurements. J. Geophys. Res. Atmos. 114.

Prakash, S., Mitra, A.K., Pai, D.S., AghaKouchak, A., 2016. From TRMM to GPM: How well can heavy rainfall be detected from space? Adv. Water Resour. https://doi.org/10.1016/j.advwatres.2015.11.008

Qin, Y., Chen, Z., Shen, Y., Zhang, S., Shi, R., 2014. Evaluation of Satellite Rainfall Estimates overtheChineseMainland. Remote Sens. 6, 11649–11672.

Roth, V., Lemann, T., 2016. Comparing CFSR and conventional weather data for discharge and soil loss modelling with SWAT in small catchments in the Ethiopian Highlands. Hydrol. Earth Syst. Sci. https://doi.org/10.5194/hess-20-921-2016

Ruan, H., Zou, S., Yang, D., Wang, Y., Yin, Z., Lu, Z., Li, F., Xu, B., 2017. Runoff simulation by SWAT model using high-resolution gridded precipitation in the upper Heihe River Basin, Northeastern Tibetan Plateau. Water (Switzerland) 9, 1–23. https://doi.org/10.3390/w9110866

Saha, S., Moorthi, S., Pan, H.L., Wu, X., Wang, Jiande, Nadiga, S., Tripp, P., Kistler, R., Woollen, J., Behringer, D., Liu, H., Stokes, D., Grumbine, R., Gayno, G., Wang, Jun, Hou, Y.T., Chuang, H.Y., Juang, H.M.H., Sela, J., Iredell, M., Treadon, R., Kleist, D., Van Delst, P., Keyser, D., Derber, J., Ek, M., Meng, J., Wei, H., Yang, R., Lord, S., Van Den Dool, H., Kumar, A., Wang, W., Long, C., Chelliah, M., Xue, Y., Huang, B., Schemm, J.K., Ebisuzaki, W., Lin, R., Xie, P., Chen, M., Zhou, S., Higgins, W., Zou, C.Z., Liu, Q., Chen, Y., Han, Y., Cucurull, L., Reynolds, R.W., Rutledge, G., Goldberg, M., 2010. The NCEP climate forecast system reanalysis. Bull. Am. Meteorol. Soc. https://doi.org/10.1175/2010BAMS3001.1

Saha, S., Moorthi, S., Wu, X., Wang, J., Becker, E., 2014. The NCEP climate forecast system version 2. J. Clim. 27, 2185–2208.

Serreze, M.C., Barrett, A.P., Lo, F., 2005. Northern High-Latitude Precipitation as Depicted by Atmospheric Reanalyses and Satellite Retrievals. Mon. Weather Rev. 133, 3407–3430.

Shakil, Ahmad, Romshoo, Reyaz, A., Dar, Irfan, Rashid, Asif, Marazi, 2015. Implications of Shrinking Cryosphere Under Changing Climate on the Streamflows in the Lidder Catchment in the Upper Indus Basin, India. Arct. Antarct. Alp. Res.

Sheng, H.U., Qiu, H., Yang, D., Cao, M., Song, J., Jiang, W.U., Huang, C., 2017. Evaluation of the applicability of climate forecast system reanalysis weather data for hydrologic simulation: A case study in the Bahe River Basin of the Qinling Mountains, China. J. Geogr. Sci. 27, 546–564.

Shuai, Z., Yimin, W., Aijun, G., Kai, Z., Ziyan, L., 2019. Influence of uncertainties in SWAT model parameters on runoff simulation in upper reaches of the Yellow River. J. Northwest A&F Univ. (Nat. Sci. Ed) 47, 144–154. https://doi.org/10.13207/j.cnki.jnwafu.2019.08.018

Sorrel, M., 2010. The NCEP Climate Forecast System Reanalysis. Bull.amer.meteor.soc 91, 1015–1057. https://doi.org/10.1175/2010BAMS3001.1

Strauch, M., Bernhofer, C., Koide, S., Volk, M., Lorz, C., Makeschin, F., 2012. Using precipitation data ensemble for uncertainty analysis in SWAT streamflow simulation. J. Hydrol. 414, 413–424.

Tang, X., Zhang, J., Wang, G., Yang, Q., Yang, Y., Guan, T., Liu, C., Jin, J., Liu, Y., Bao, Z., 2019. Evaluating Suitability of Multiple Precipitation Products for the Lancang River Basin. Chinese Geogr. Sci. 29, 37–57. https://doi.org/10.1007/s11769-019-1015-5

Tekeli, A.E., Fouli, H., 2016. Evaluation of TRMM satellite-based precipitation indexes for flood forecasting over Riyadh City, Saudi Arabia. J. Hydrol. 471–479.

Tian, Y., Peters-Lidard, C.D., 2010. A global map of uncertainties in satellite-based precipitation measurements. Geophys. Res. Lett. 37.

Tuo, Y., Duan, Z., Disse, M., Chiogna, G., 2016. Evaluation of precipitation input for SWAT modeling in Alpine catchment: A case study in the Adige river basin (Italy). Sci. Total Environ. 573, 66–82. https://doi.org/10.1016/j.scitotenv.2016.08.034

Villaran, L.G.O.I.C.C.F. de, 2014. Rainfall estimation in SWAT: An alternative method to simulate orographic precipitation. J. Hydrol. 509, 257–265.

Villarini, G., Krajewski, W.F., Smith, J.A., 2009. New paradigm for statistical validation of satellite precipitation estimates: Application to a large sample of the TMPA 0.25deg 3-hourly estimates over Oklahoma. J. Geophys. Res. Atmos. 114.

Viviroli, D., Weingartner, R., 2004. The hydrological significance of mountains: from regional to global scale. Hydrol. Earth Syst. Sci. 8.

Wang, N., Liu, Wenbin, Sun, F., Yao, Z., Wang, H., Liu, Wanqing, 2020. Evaluating satellite-based and reanalysis precipitation datasets with gauge-observed data and hydrological modeling in the Xihe River Basin, China. Atmos. Res. 234. https://doi.org/10.1016/j.atmosres.2019.104746

Wu, Z., Du, H., Zhao, D., Li, M., Meng, X., Zong, S., 2012. Estimating daily global solar radiation during the growing season in Northeast China using the ngstrm–Prescott model. Theor. Appl. Climatol. 108, 495–503.

Xu, Z., He, W., 2006. Spatial and Temporal Characteristics and Change Trend of Climatic Elements in the Headwater Region of the Yellow River in Recent 40 Years. Plateau Meteoro Logy 25, 906–913. https://doi.org/10.1016/S1003-6326(06)60040-X (In Chinese)

Yan, L., Di, L., Liangliang, B., Caijin, Z., Zhongying, H., Xingdong, L., Wen, W., Shaohong, S., Yuntao, Y., 2020. A review on water resources stereoscopic monitoring systems based on multisource data. J. Remote Sensing(Chinese) 24, 787–803. https://doi.org/10.11834/jrs.20200123

Yang, M., Liu, G., Chen, T., Chen, Y., Xia, C., 2020. Evaluation of GPM IMERG precipitation products with the point rain gauge records over Sichuan, China. Atmos. Res. 246, 105101. https://doi.org/10.1016/j.atmosres.2020.105101

Yong, B., Chen, B., Gourley, J.J., Ren, L., Hong, Y., Chen, X., Wang, W., Chen, S., Gong, L., 2014. Intercomparison of the Version-6 and Version-7 TMPA precipitation products over high and low latitudes basins with independent gauge networks: Is the newer version better in both real-time and post-real-time analysis for water resources and hydrologic extr. J. Hydrol. 508, 77–87.

Yuan, F., Berndtsson, R., Zhang, L., Uvo, C.B., Hao, Z., Wang, X., Yasuda, H., 2015. Hydro climatic trend and periodicity for the source region of the Yellow river. J. Hydrol. Eng. https://doi.org/10.1061/(ASCE)HE.1943-5584.0001182

Yuan, F., Wang, B., Shi, C., Cui, W., Zhao, C., Liu, Y., Ren, L., Zhang, L., Zhu, Y., Chen, T., Jiang, S., Yang, X., 2018. Evaluation of hydrological utility of IMERG Final run V05 and TMPA 3B42V7 satellite precipitation products in the Yellow River source region, China. J. Hydrol. https://doi.org/10.1016/j.jhydrol.2018.06.045

Yw, A., Lga, B., Hz, C., Bing, Z.A., Mld, A., 2019. Hydroclimate assessment of gridded precipitation products for the Tibetan Plateau. Sci. Total Environ. 660, 1555–1564.

Zhang, L., Meng, X., Wang, H., Yang, M., Cai, S., 2020. Investigate the applicability of CMADS and CFSR reanalysis in Northeast China. Water (Switzerland). https://doi.org/10.3390/W12040996

Zhenchun, H., Yueguan,Zhang, Chuanguo,Yang, Jiawei,Li, Thondup, D., 2013. Effects of topography and snowmelt on hydrologic simulation in the Yellow River's source region. Adv. Water Sci. Methodol. 24, 311–318. https://doi.org/10.14042/j.cnki.32.1309.2013.03.018

Zhu, Q., Xuan, W., Liu, L., Xu, Y.P., 2016. Evaluation and hydrological application of precipitation estimates derived from PERSIANN-CDR, TRMM 3B42V7, and NCEP-CFSR over humid regions in China. Hydrol. Process. 30, 3061–3083. https://doi.org/10.1002/hyp.10846

Zhu, X., Zhang, M., Wang, S., Qiang, F., Zeng, T., Ren, Z., Dong, L., 2015. Comparison of monthly precipitation derived from high-resolution gridded datasets in arid Xinjiang, central Asia. Quat. Int. 358, 160–170.

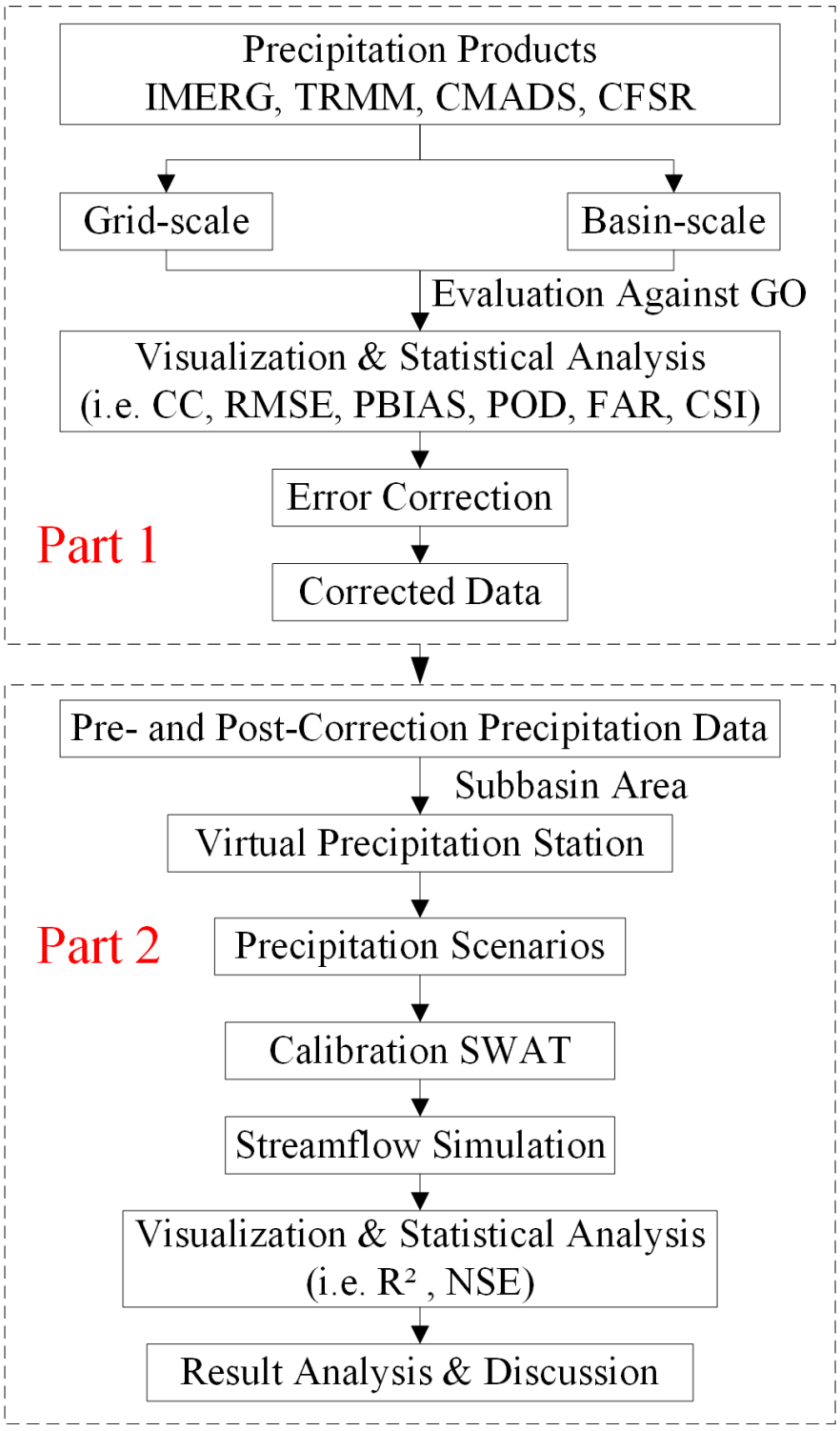

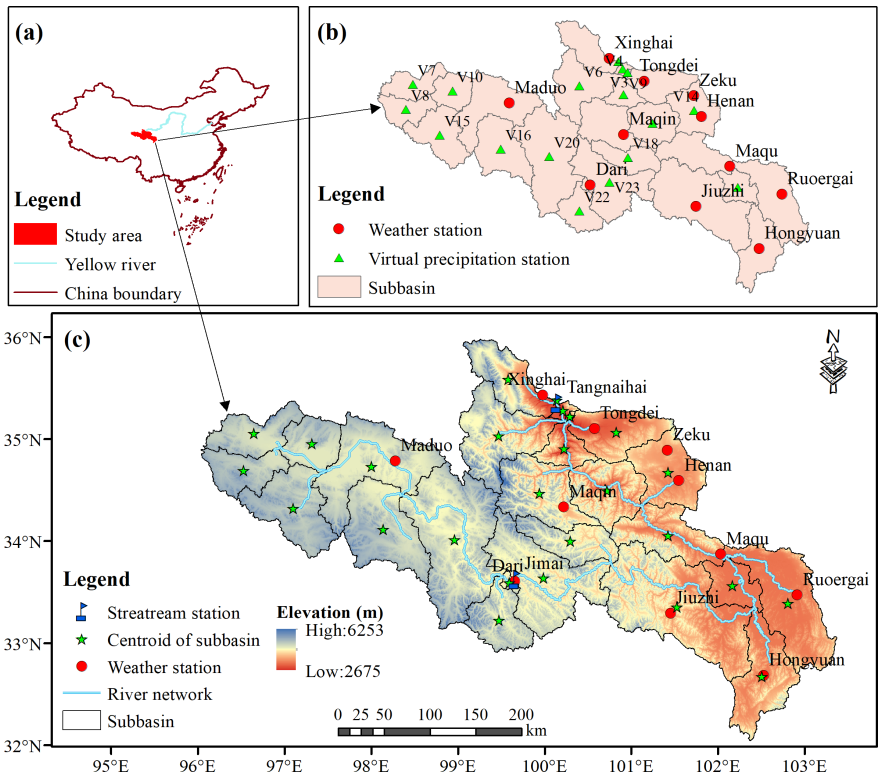

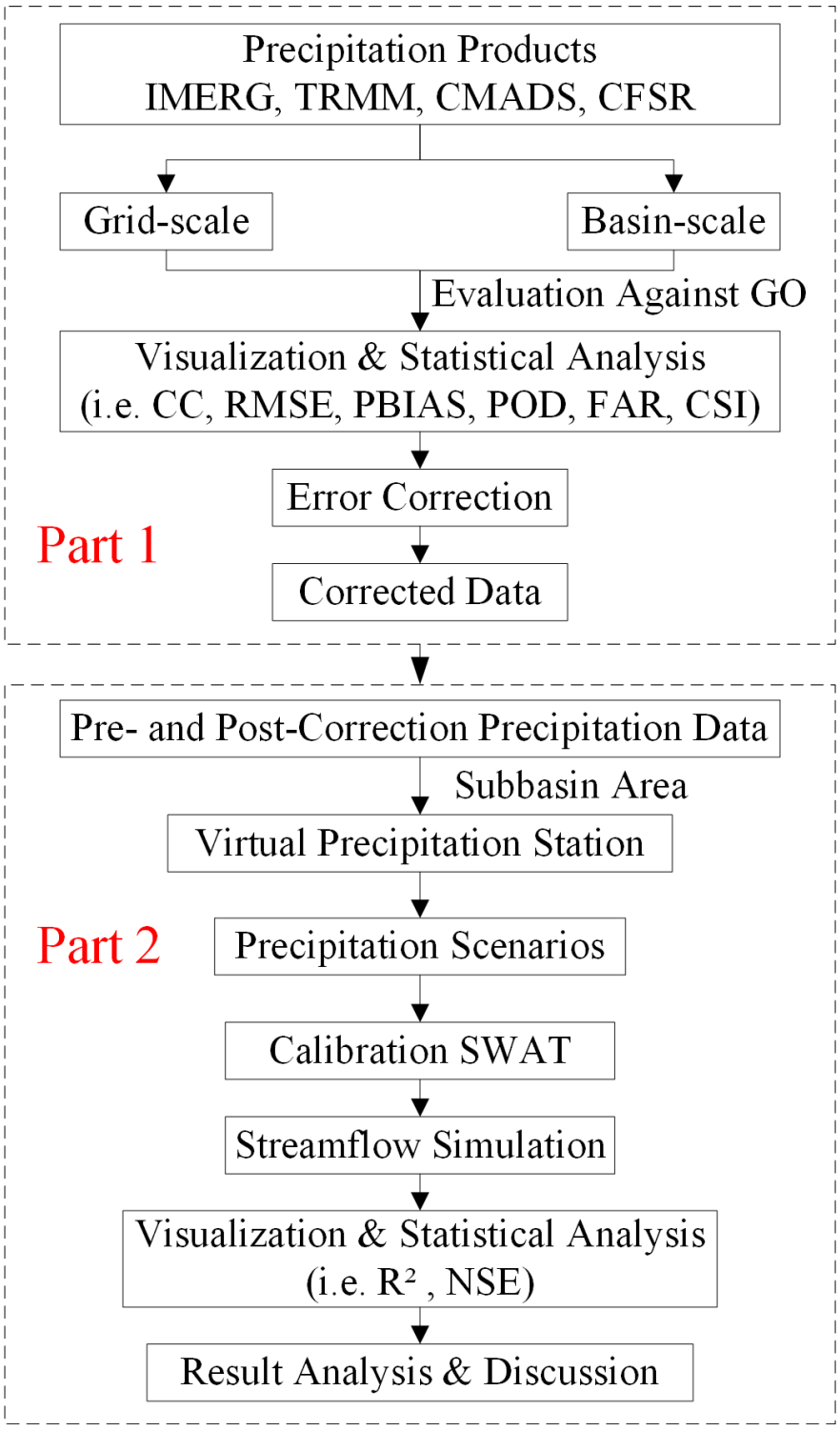

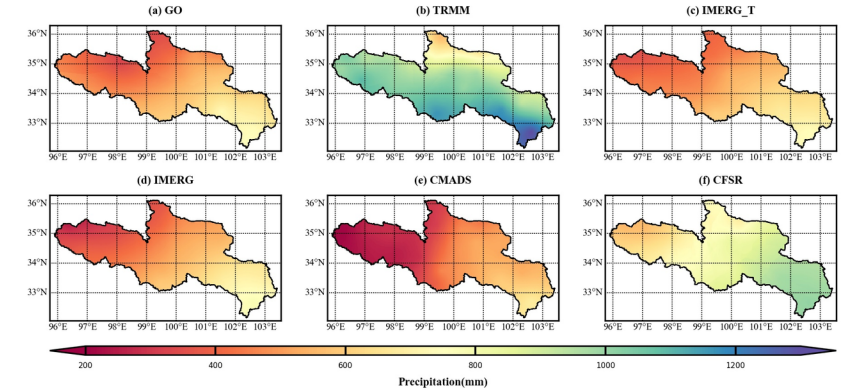

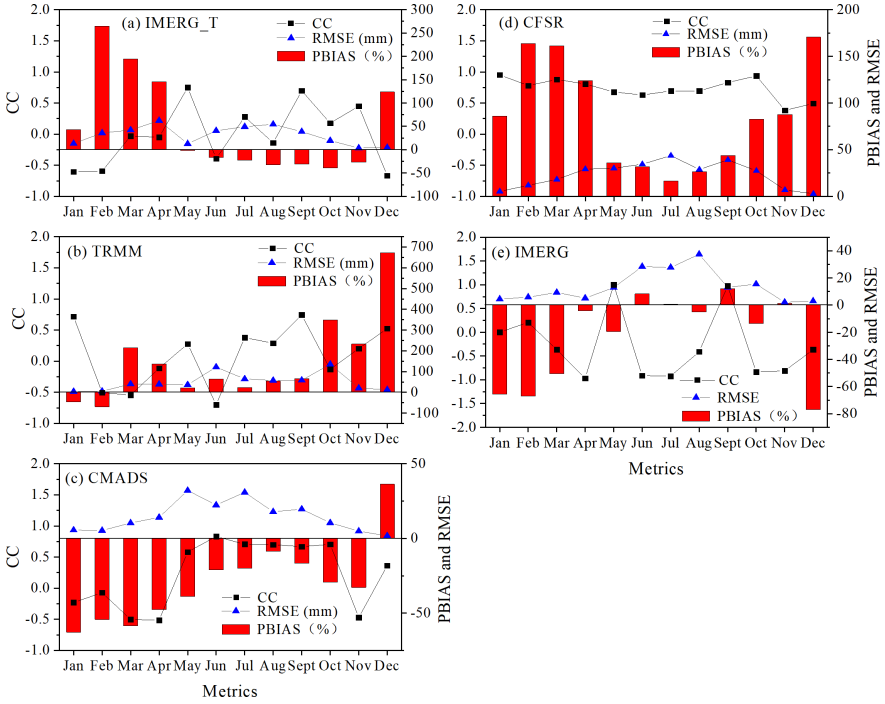

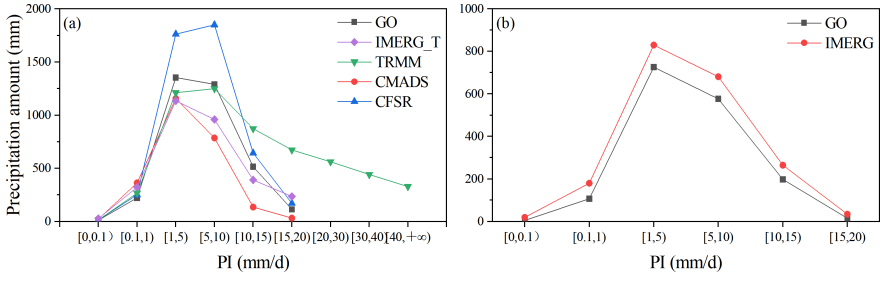

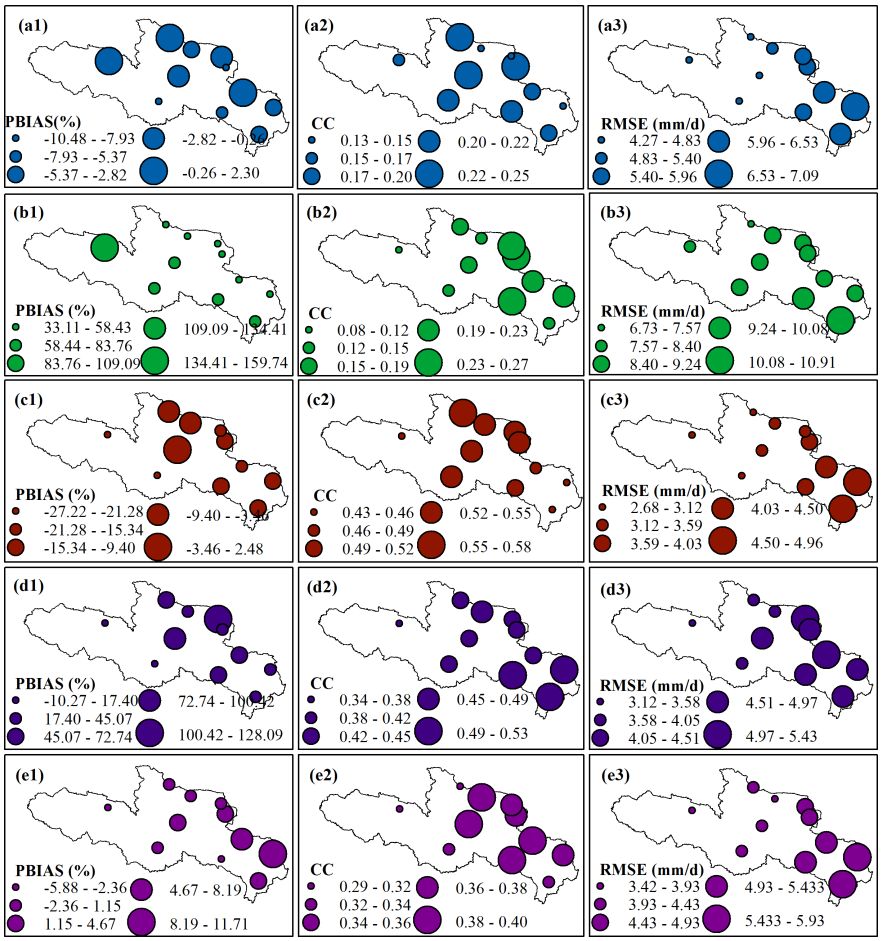

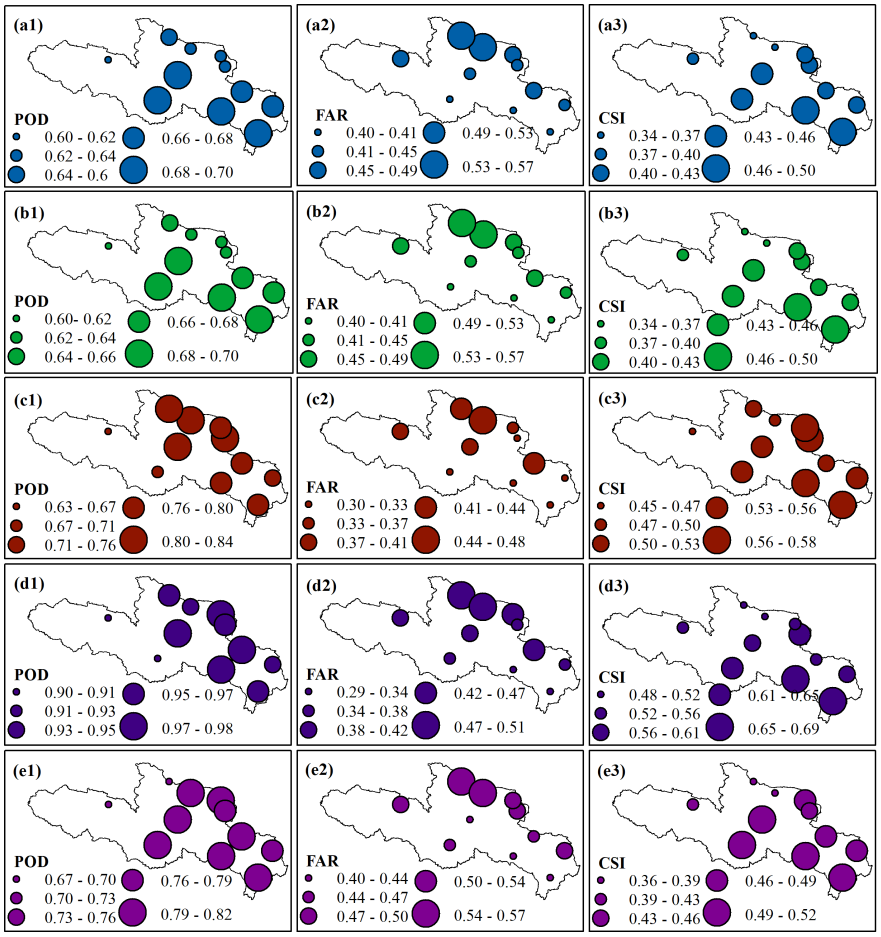

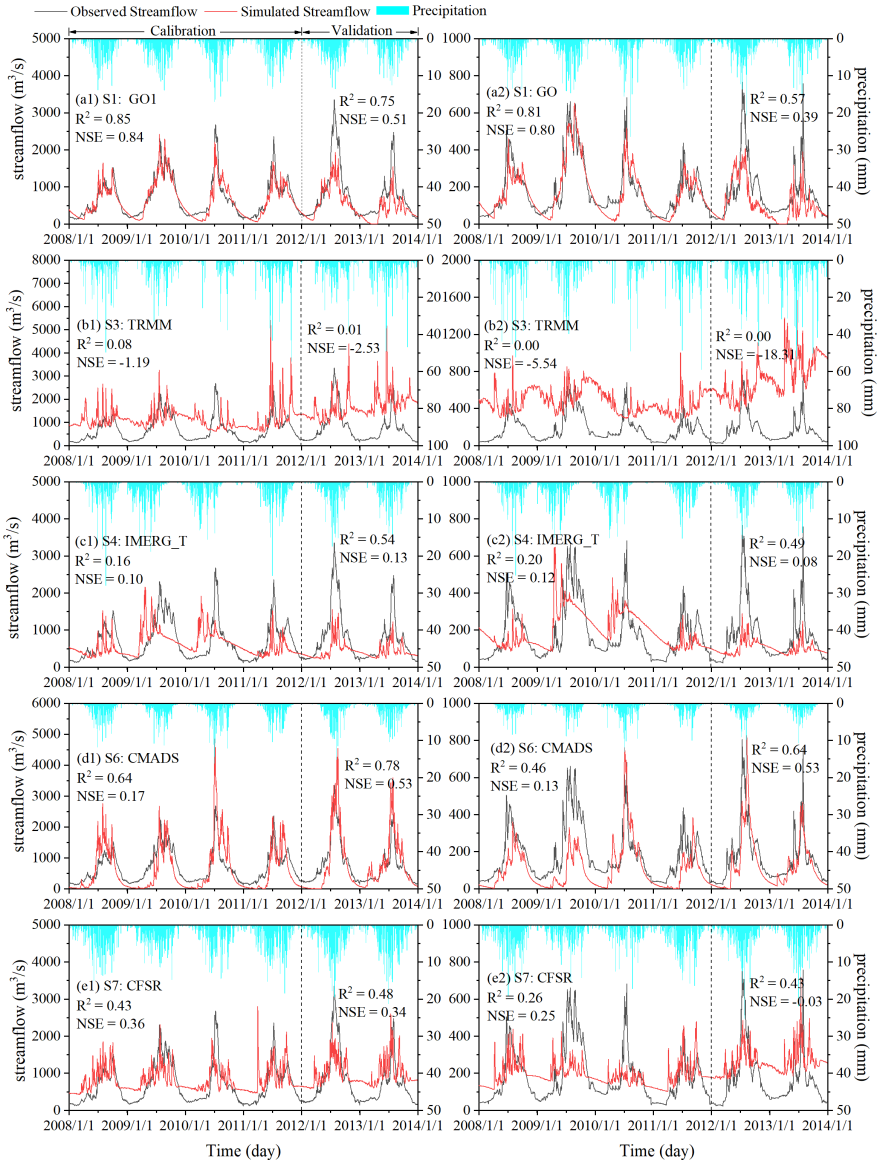

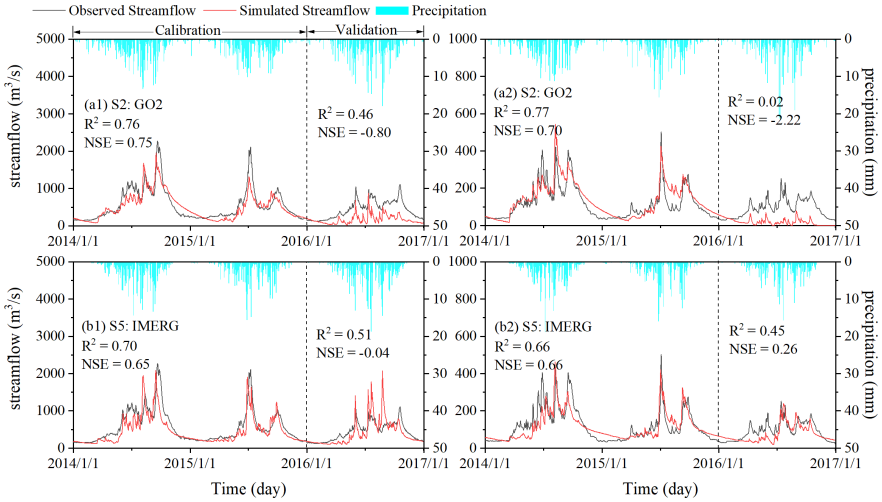

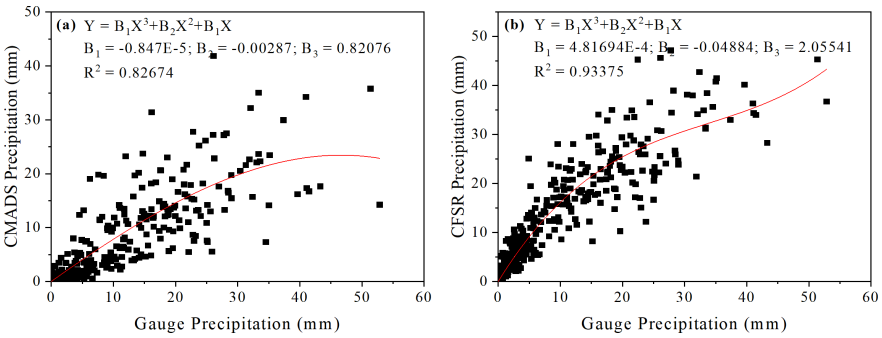

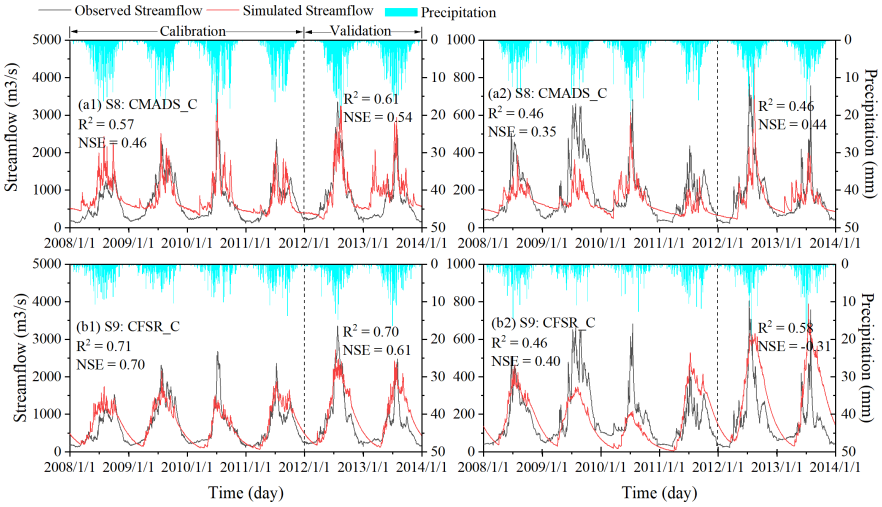

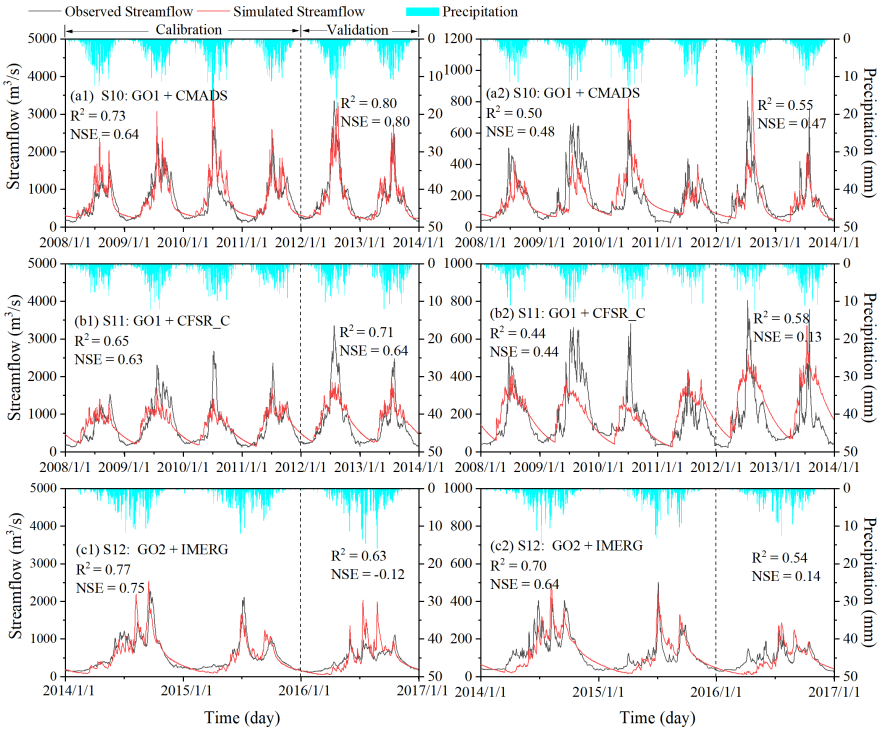

Hosted file

Table 1.docx available at https://authorea.com/users/360620/articles/538482-evaluation-of-multisource-precipitation-input-for-hydrological-modeling-in-an-alpine-basin-a-case-study-from-the-yellow-river-source-region-china

Hosted file

Table 2.docx available at https://authorea.com/users/360620/articles/538482-evaluation-of-multisource-precipitation-input-for-hydrological-modeling-in-an-alpine-basin-a-case-study-from-the-yellow-river-source-region-china

Hosted file

Table 3.docx available at https://authorea.com/users/360620/articles/538482-evaluation-of-multisource-precipitation-input-for-hydrological-modeling-in-an-alpine-basin-a-case-study-from-the-yellow-river-source-region-china

Hosted file

Table 4.docx available at https://authorea.com/users/360620/articles/538482-evaluation-of-multisource-precipitation-input-for-hydrological-modeling-in-an-alpine-basin-a-case-study-from-the-yellow-river-source-region-china

Hosted file

Table 5.docx available at https://authorea.com/users/360620/articles/538482-evaluation-of-multisource-precipitation-input-for-hydrological-modeling-in-an-alpine-basin-a-case-study-from-the-yellow-river-source-region-china